Integrated Optical Coherent Balanced Receiver

P. S. Cho, G. Harston, A. Greenblatt, and A. Kaplan
CeLight, Inc., 12200 Tech Road, Suite 300, Silver Spring, MD 20904, USA.   E-mail: pscho@celight.com
Y. Achiam, R. M. Bertenburg, and A. Brennemann
synQPSK Consortium, Univ. Paderborn, EIM-E, Opt. Com. & High-Freq. Engineering, Warburger Str. 100, D-33098, Paderborn, Germany
B. Adoram, P. Goldgeier, and A. Hershkovits
Elisra Group, 48 Mivtza Kadesh St., Bene Beraq 51203, Israel

Abstract: A 1550-nm coherent receiver with a $LiNbO_3$ optical hybrid and balanced photoreceivers integrated in a single compact package is reported. Frequency response of the integrated receiver and bit-error-rate measurements of optical PSK signals are described.
©2006 Optical Society of America
OCIS codes: (060.1660) Coherent communications; (250.3140) Integrated optoelectronic circuits

1. Introduction

A coherent receiver typically employs an optical hybrid followed by balanced photoreceivers at the front end. The optical hybrid combines the signal and a local laser before mixing at the photodetectors. An integrated $LiNbO_3$ based optical hybrid has been previously reported and shown to be a robust device for homodyne [1] as well as differential detection [2]. As the signal's symbol rate increases, tolerance of path length mismatch in the connecting optical fibers between the optical hybrid and the balanced detectors reduces [1]. This calls for the need of an integrated device in which the photodetectors are precisely mounted at the outputs of the optical hybrid eliminating connecting fibers and thus the associated coupling losses and length mismatch. We describe here, to our knowledge, the first integration of a 6-port $LiNbO_3$ optical hybrid and two sets of balanced photoreceivers with high-gain transimpedance amplifiers (TIAs) in a single compact fiber-pigtailed package. Conversion gain frequency response of the packaged integrated coherent receiver (ICR) as well as bit-error-rate (BER) measurement of optical phase-shift-keyed (PSK) signals using the ICR are presented.

2. Integrated coherent receiver

Fig. 1 shows a schematic of the ICR and a photograph of the packaged device with polarization-maintaining (PM) input fibers. The $LiNbO_3$ optical hybrid is based on x-cut Ti-diffused waveguides with four interconnecting directional couplers and two phase-shifters all voltage controllable [1]. A PM-fiber V-groove array was used to couple light into the $LiNbO_3$ waveguides of the optical hybrid. The optical excess loss due to waveguide and coupling losses of the ICR is about -4.35 dB. Reduction of the excess loss to around -1.5 dB is possible and is expected in the next-generation device. The balanced photoreceiver, mounted on a specially designed submount, is consists of a linear array of InP photodiodes and two commercial TIAs with differential outputs (positive/negative). The photodiodes and TIAs are mounted and connected together via a specially designed high-speed micro-circuit board.
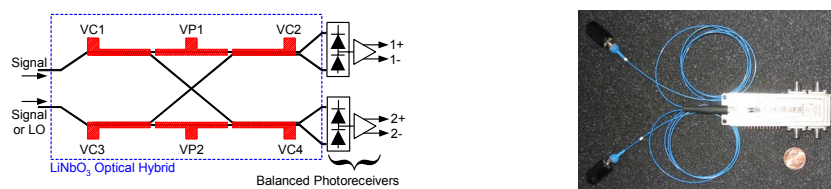
Fig. 1. Left: Schematic of the 6-port optical hybrid and balanced photoreceiver pairs. VC1 to VC4 are the coupler electrodes while VP1 and VP2 are the phase electrodes. Right: photograph of the ICR. Dimensions: $127 \times 26 \times 13$ mm^3.

The responsivity of the photodiode at 1550 nm is about 0.9 A/W and the typical dark current is about 30 nA. Fig. 2a shows the small-signal conversion gain (C_g) frequency response of the four RF ports of the ICR including the excess loss (-4.35 dB). C_g without excess loss is therefore higher as can be seen in Fig. 2b. As shown in Fig. 2a, C_g is about 250 V/W near 8 GHz but drops off to below 100 V/W beyond 12 GHz. This can be attributed to the combined frequency response of the photodetector and TIA before packaging as shown in Fig. 2b (excess loss removed) where the response drops sharply near 10 GHz, which accounts for the frequency response roll-off of the ICR beyond 10 GHz. C_g of the 1- port of the ICR without excess loss is also shown in Fig. 2b. The additional bandwidth reduction of the ICR is attributed to parasitics of the micro-circuit board that will be optimized in the next-generation device.
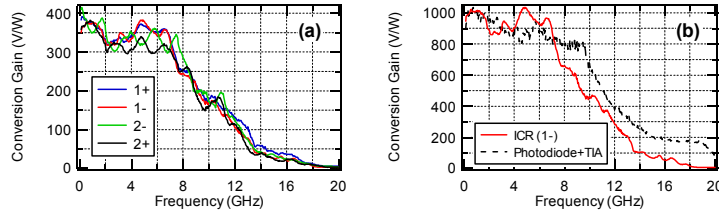
Fig. 2. (a) Conversion gain frequency response of the four RF ports of the ICR with excess loss included. (b) Combine response of the photodiode and the TIA (before packaging) and the ICR response (1-) with excess loss removed.

3. Detection of optical PSK signal

The ICR was used to detect optical PSK signals of different formats and symbol rates for system performance evaluation. Error-free (BER < 10^{-9}) detection of a 8-GSym/s differential binary PSK (DBPSK) signal using the ICR with optical pre-amp and filtering at the receiver employing differential detection was achieved as can be seen in Fig. 3. The 8-GSym/s DBPSK signal was produced by a Mach-Zehnder modulator (MZM) biased at null and driven by a 8 Gb/s non-return-to-zero (NRZ) pseudo-random binary sequence (PRBS) with a word length of 2^{15}-1.
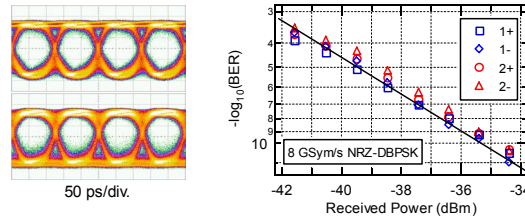
Fig. 3. Left: eye waveforms of detected 8 GSym/s NRZ-DBPSK signal from 1+ port of ICR. Vertical scale: 100 mV/div.
Right: Measured BER of the four RF ports of the ICR versus received power.

The performance of ICR using 12.5 GSym/s return-to-zero (RZ) differential quaternary PSK (DQPSK) signal was evaluated using the receiver setup shown in Fig. 4. The RZ-DQPSK signal at ~ 1545 nm was produced by driving a packaged LiNbO$_3$ quadrature optical modulator with two 12.5 Gb/s NRZ PRBS (word length: 2^{15}-1) signals followed by a MZM pulse carver driven at 12.5 GHz producing 50% duty cycle pulse train. The two NRZ signals are complementary with a 2-symbol relative time delay. No differential encoding was used. The LiNbO$_3$ quadrature modulator was also fabricated and packaged in-house. Details of the quadrature modulator will be presented. The RZ-DQPSK signal was directed to an erbium-doped fiber amplifier (EDFA) via a variable optical attenuator (VOA1) to control optical power into the EDFA. A 47-GHz optical bandpass filter (BPF) was used to suppress ASE noise. A polarization controller (PC) and a polarization beam splitter (PBS) were used to ensure that the correct polarization is launched into the ICR. A PM 3-dB coupler and a variable optical delay line (VDL) were connected to the two inputs of the ICR providing the one-symbol-delay (80 ps) for differential detection as shown in Fig. 4. Due to the high insertion loss of the VDL (-8 dB), an attenuator (VOA3) was inserted into the other arm to balance the loss. As a result, the maximum optical power available at the input fiber of the ICR was about -1 dBm (EDFA saturated). RF outputs of the ICR were connected to a sampling oscilloscope for eye waveform monitoring or to an error detector for BER measurement. One of the RF ports of the ICR was directed to a phase control loop used to maintain optimal phase shift in the hybrid (via VP1 or VP2) for maximum eye opening [1]. DC voltages were applied to the ICR for photodiodes biases, powering the TIAs, and biasing the couplers (VC1 to VC4).
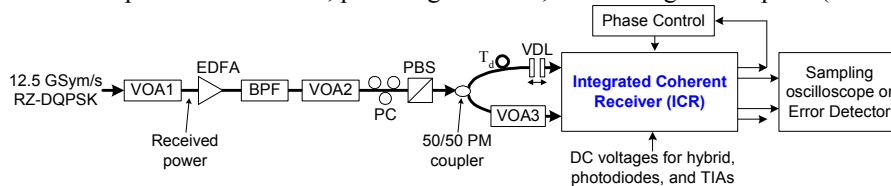
Fig. 4. Detection of 12.5 GSym/s RZ-DQPSK signal using the ICR with closed-loop phase control. T_d = 80 ps.

Fig. 5 shows eye diagrams and BER measurement results of the in-phase (I) and quadrature-phase (Q) components of the detected 12.5 GSym/s RZ-DQPSK signal. Error-free detection was not possible in this case. This is attributed to the frequency response of the ICR beyond 10 GHz and the high insertion loss of the VDL in contrast to the case of 8-GSym/s DBPSK error-free detection, which did not require a VDL. Nevertheless, with advanced

forward-error-correction (FEC) coding, a corrected BER less than 10^{-12} is expected for 20 Gb/s aggregated data rate since the symbol rate included 25% overhead bandwidth [2]. The received power required for uncorrected BER of 10^{-3} (FEC threshold) is about -34 dBm including insertion loss of the VDL. As a comparison, the ICR was replaced with discrete components (DCs): a packaged 6-port LiNbO$_3$ optical hybrid (excess loss: -3.7 dB) and a commercial 15-GHz balanced photoreceiver [2]. BER performance using DCs is also shown in Fig. 5, which is inferior to ICR. This can be attributed to the significantly higher conversion gain of the ICR. Note that the BER performance for both ICR and DCs is expected to improve significantly if the insertion loss of the VDL is eliminated.

ICR (-26.7 dBm)   DCs (-15.6 dBm)
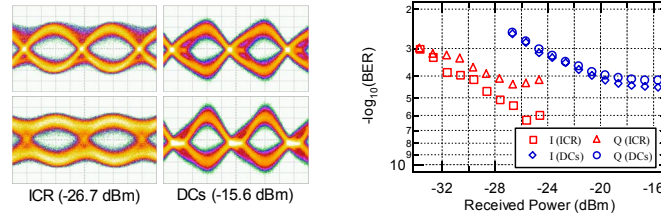
Fig. 5. Left: eye diagrams of I (top) and Q (bottom) components of detected 12.5 GSym/s RZ-DQPSK from RF port 2- of the ICR and from discrete components (DCs). Received powers are shown in parenthesis. Horizontal scale: 20 ps/div. Right: BER vs. received optical power of I and Q components of RZ-DQPSK using ICR (RF port: 2-) and DCs.

Self-homodyne detection of a 12.5 GSym/s BPSK signal using the ICR was investigated with the local laser oscillator (LO) derived from the transmitting laser to achieve automatic phase locking as shown in Fig. 6. BER $< 10^{-9}$ can be obtained with a received power of -25 dBm at the input fiber of the ICR and a LO optical power of +9.75 dBm. The eye diagram of the detected BPSK signal from 1+ port of the ICR for -25 dBm received power is shown in the top right of Fig. 6. As a comparison, the ICR was replaced with discrete components (DCs) as described earlier. In this case, a higher received power of -7 dBm and a LO power of +9.75 dBm were required to achieve a BER of 10^{-9}. The eye waveform of the detected BPSK signal using DCs for -25 dBm received power is shown in the bottom right of Fig. 6. Here again, the ICR significantly outperforms DCs as a result of its high sensitivity (conversion gain) and high saturation power, which is crucial for coherent homodyne detection.
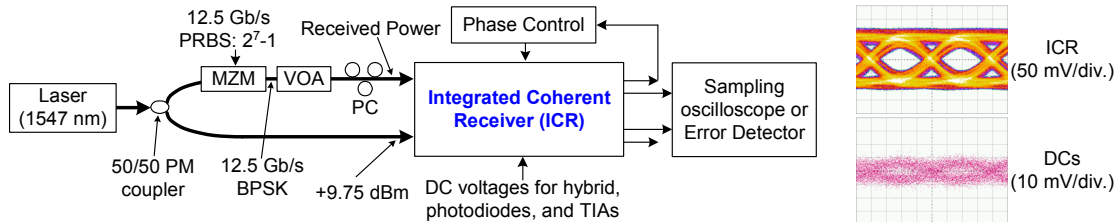
Fig. 6. Self-homodyne detection of 12.5 Gb/s BPSK using ICR. Eye waveforms of detected 12.5 GSym/s BPSK using ICR (top right) and discrete components (bottom right) for received power of -25 dBm are shown. Horizontal scale: 20 ps/div.

In summary, a compact packaged ICR consisting of a LiNbO$_3$ optical hybrid and a pair of balanced photoreceivers is reported for the first time to the best of our knowledge. The ICR has a high conversion gain and a RF bandwidth around 8 GHz and rolls off sharply near 10 GHz primarily due to the photodiode and TIA. Error-free detection of 8 GSym/s optical DBPSK signal were achieved with a receiver sensitivity less than -36 dBm at 10^{-9} BER using an optical pre-amp. Detection of a 12.5-GSym/s RZ-DQPSK signal using the ICR was investigated. The BER performance was primarily limited by the receiver setup (high insertion loss of VDL) and the frequency response of the ICR beyond 10 GHz. Nevertheless, the ICR compares favorably to discrete components. We have also investigated self-homodyne detection of 12.5 GSym/s BPSK signal using the ICR and DCs. The ICR shows much higher detection sensitivity (-25 dBm) than DCs (-7 dBm) due to its high conversion gain and high saturation power. The frequency response of the next-generation ICR is expected to improve with better components (e.g., photodiodes and TIAs) and optimization of the micro-circuit board.

References

[1] P. S. Cho, et al., "Coherent homodyne detection of BPSK signals using time-gated amplification and LiNbO$_3$ optical 90° hybrid," Photon. Technol. Lett., **16**, 1727-1729 (2004).

[2] P. S. Cho, et al., "Investigation of 2-bit/s/Hz 40-Gb/s DWDM transmission over 4×100-km SMF-28 fiber using RZ-DQPSK and polarization multiplexing," Photon. Technol. Lett., **16**, 656-658 (2004).